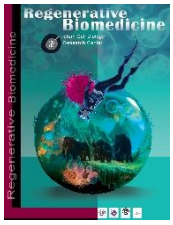

Regenerative Biomedicine

Production and Hosting: Shahid Sadoughi University of Medical Sciences

Journal homepage: jrb.ssu.ac.ir

Original Article

Niosome-Encapsulated *Withania somnifera (Ashwagandha)* Extract Enhances Apoptosis in Cervical Cancer HeLa Cells via Modulation of BCL-2 and p53 Gene Expression

Mahdieh Marvasti [1], Narges Nikoonahad Lotfabadi [1*], Bibi Fatemeh Haghiralsadat [2]

1- Department of Biology, Science Faculty, Science and Arts University, Yazd, Iran.
2- Stem Cell Biology Research Center, Yazd Reproductive Sciences Institute, Shahid Sadoughi University of Medical Sciences, Yazd, Iran.

***Corresponding Author:**
Nikonahad Lotfabadi, Narges

Email:
nikonahad@gmail.com

Received:
2026-05-12
Accepted:
2026-06-02

Volume:2
Issue no.1

Editor-in-Chief:

Behrouz Aflatoonian Ph.D.

Abstract

Cervical cancer is the fourth most common cancer and leading cause of cancer-related mortality among women worldwide. Conventional treatments including surgery, radiotherapy, and chemotherapy are often associated with severe adverse effects that limit their clinical use. Nanotechnology-based drug delivery systems offer a promising strategy to overcome these therapeutic limitations. Niosome nanoparticles encapsulating *Withania somnifera (Ashwagandha)* extract were synthesized via thin-film hydration using Span-60 and cholesterol (70:30 molar ratio). Characterization included dynamic light scattering, FTIR, and UV-Vis spectrophotometry. Cytotoxicity was evaluated by MTT assay in HeLa and HFF cell lines. *BCL2* and *TP53* gene expression was assessed by Real-Time PCR. The optimized formulation showed 69 ± 2.8% encapsulation efficiency, 101.2 nm mean particle size, 0.429 PDI, and −24.1 mV zeta potential. Drug release exhibited biphasic kinetics with 60.7% cumulative release at 72 hours. The IC_{50} against HeLa cells was 168 µg/mL, significantly lower than free extract (257.9 µg/mL). The niosomal formulation significantly upregulated *TP53* and downregulated *BCL2* expression compared to controls ($P < 0.05$), with negligible toxicity to normal HFF cells. Niosomal encapsulation substantially enhances Ashwagandha's anticancer efficacy against cervical cancer cells while maintaining normal cell viability, representing a promising biocompatible nanoplatform for targeted therapy.

Keywords: Apoptosis, Cervical cancer, Nanoparticle drug delivery, *Withania somnifera*

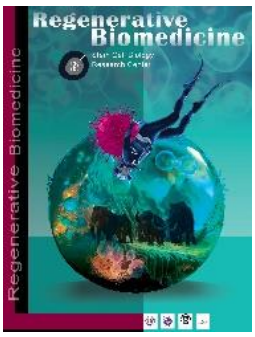

How to cite this article:
Marvasti, M., Nikonahad Lotfabadi, N., Haghiralsadat, BF. Niosome-Encapsulated *Withania somnifera (Ashwagandha)* Extract Enhances Apoptosis in Cervical Cancer HeLa Cells via Modulation of BCL-2 and p53 Gene Expression. *Regenerative Biomedicine*, 2026; 2(1): 1-19. https://doi.org/10.22034/jrb.2026.07.V2I1A1

Introduction

Cervical cancer remains one of the most prevalent gynecological malignancies worldwide, ranking as the fourth most common cancer among women (1). In 2018, approximately 570,000 new cases and 311,000 deaths were reported globally, with the majority occurring in low- and middle-income countries (2). The primary etiological agent of cervical cancer is persistent infection with high-risk human papillomavirus (HPV) types, particularly HPV-16 and HPV-18, which account for approximately 70% of all cervical cancer cases (3). The viral oncoproteins E6 and E7 play a critical role in cervical carcinogenesis by inactivating the tumor suppressor proteins p53 and retinoblastoma (Rb), respectively, leading to uncontrolled cell proliferation and inhibition of apoptosis (4). The E6 protein binds to p53 and promotes its ubiquitin-mediated degradation, thereby preventing p53-induced cell cycle arrest and apoptosis (5). Current treatment modalities for cervical cancer include surgery, radiotherapy, chemotherapy, and concurrent chemoradiotherapy, depending on the stage and extent of the disease (6). However, conventional treatments are associated with significant side effects, including fatigue, nausea, vomiting, bone marrow suppression, and damage to surrounding healthy tissues (7). Moreover, the development of multidrug resistance (MDR) remains a major challenge in the treatment of cervical cancer, limiting the efficacy of chemotherapeutic agents and contributing to treatment failure and disease recurrence (8). The molecular mechanisms underlying cervical cancer progression involve dysregulation of key signaling pathways that control cell proliferation, apoptosis, and survival. One of the most critical pathways is the intrinsic apoptotic pathway, which is regulated by the B-cell lymphoma 2 (BCL-2) family of proteins (9). Overexpression of anti-apoptotic BCL-2 proteins has been observed in various cancers, including cervical cancer, and is associated with resistance to chemotherapy and poor prognosis (10). Therefore, targeting BCL-2 family proteins represents a promising therapeutic strategy for overcoming apoptosis resistance in cervical cancer. Another critical molecular target in cervical cancer is the tumor suppressor protein p53, which plays a central role in maintaining genomic stability and regulating cell cycle checkpoints, DNA repair, and apoptosis (11). As mentioned earlier, HPV E6 oncoprotein promotes the degradation of p53, thereby abrogating its tumor suppressor functions and contributing to malignant transformation. Restoration of p53 function or inhibition of its degradation has been proposed as a potential therapeutic approach for cervical cancer. In recent years, there has been growing interest in the use of natural products and herbal medicines as alternative or complementary therapies for cancer treatment (12). Many plant-derived compounds have demonstrated anticancer properties through multiple mechanisms, including induction of apoptosis, inhibition of cell proliferation, modulation of signaling pathways, and enhancement of immune responses (13). One such medicinal plant with promising anticancer potential is *Withania somnifera*, commonly known as Ashwagandha or Indian ginseng (14). *Withania somnifera* is a small shrub belonging to the Solanaceae family and is native to India, the Middle East, and parts of Africa (15). It has been extensively used in

https://doi.org/10.22034/jrb.2026.07.V2I1A1

Ayurvedic medicine for its adaptogenic, anti-inflammatory, antioxidant, immunomodulatory, and anticancer properties (16). The plant contains a variety of bioactive compounds, including withanolides, alkaloids, saponins, and flavonoids, with withanolides being the most pharmacologically active constituents (17). Withanolides are a group of naturally occurring steroidal lactones that have been shown to exhibit potent anticancer effects against various cancer cell lines, including breast, lung, colon, prostate, and cervical cancer (18). Despite the promising anticancer properties of *Withania somnifera* extracts, their clinical application is limited by several pharmacokinetic challenges, including poor aqueous solubility, low bioavailability, rapid metabolism, and non-specific distribution (19). These limitations necessitate the development of advanced drug delivery systems that can enhance the solubility, stability, and targeted delivery of herbal extracts to cancer cells while minimizing systemic toxicity. Nanotechnology has emerged as a powerful tool for overcoming the limitations of conventional drug delivery systems (20). Nanoparticle-based drug delivery systems offer several advantages, including improved drug solubility and stability, controlled and sustained release, enhanced cellular uptake, and the ability to target specific tissues or cells (21). Niosomes are non-ionic surfactant-based vesicular systems that have gained considerable attention as drug delivery carriers due to their unique properties (22). Niosomes are self-assembled vesicles composed of non-ionic surfactants and cholesterol, which form bilayer structures similar to liposomes (23). Compared to liposomes, niosomes offer several advantages, including greater chemical stability, lower cost, ease of preparation and storage, and the ability to encapsulate both hydrophilic and hydrophobic drugs (24). Niosomes have been successfully used for the delivery of various therapeutic agents, including anticancer drugs, antibiotics, anti-inflammatory agents, and herbal extracts (25-28). Additionally, niosomes can be designed to be pH-sensitive, allowing for controlled drug release in the acidic tumor microenvironment (29, 30). The present study aims to develop and characterize niosomal nanoparticles loaded with *Withania somnifera* extract for the treatment of cervical cancer. The specific objectives of this study are: (1) to synthesize and optimize niosomal formulations using different ratios of non-ionic surfactants and cholesterol; (2) to characterize the physicochemical properties of the niosomes, including particle size, polydispersity index, zeta potential, encapsulation efficiency, and morphology; (3) to evaluate the in vitro drug release profile under different pH conditions; (4) to assess the cytotoxic effects of the niosomal formulation against HeLa cervical cancer cells and normal cells; and (5) to investigate the molecular mechanisms of action by analyzing the expression of *BCL2* and *TP53* genes. By encapsulating *Withania somnifera* extract in niosomes, we hypothesize that the bioavailability, stability, and selective cytotoxicity of the herbal extract will be significantly enhanced, leading to improved therapeutic efficacy against cervical cancer cells.

Materials and Methods

Materials

Span-60 (sorbitan monostearate), cholesterol, chloroform, isopropanol, phosphate-buffered saline (PBS, pH 7.4), and dimethyl sulphoxide (DMSO) were obtained from Sigma-Aldrich (USA). Ashwagandha *(Withania somnifera)* root extract was procured from a certified commercial supplier. MTT (3-(4,5-dimethylthiazol-2-yl)-2,5-diphenyltetrazolium bromide) reagent and cell culture materials (DMEM, foetal bovine serum (FBS), L-glutamine, penicillin-streptomycin) were obtained from Gibco (Thermo Fisher Scientific, USA). HeLa (ATCC CCL-2) and HFF (human foreskin fibroblast) cell lines were provided by the Pasteur Institute of Iran and the Yazd Infertility Center, respectively. All reagents were of analytical grade.

Niosome Synthesis (Thin-Film Hydration Method)

Niosome nanoparticles encapsulating Ashwagandha extract were prepared by the thin-film hydration (TFH) method, a reproducible and scalable technique for vesicle production (31). Briefly, Span-60 and cholesterol were dissolved in chloroform at a molar ratio of 70:30 with a total lipid concentration of 2 mg/mL in a round-bottomed flask. The organic solvent was removed by rotary evaporation (Heidolph, Germany) at 40°C under reduced pressure, generating a thin, uniform lipid film on the inner flask wall. The dried film was hydrated with 10 mL of phosphate-buffered saline (PBS, pH 7.4) containing 2 mg/mL Ashwagandha extract at 45°C for 60 minutes with gentle agitation, resulting in the spontaneous formation of multilamellar vesicles (32). The resulting multilamellar suspension was subjected to probe sonication (60 W, 30 min; 15 s on / 10 s off cycles; tip immersed in an ice bath) to reduce vesicle size and produce small unilamellar niosomes. The dispersion was subsequently extruded through a 200 nm polycarbonate membrane filter to achieve size uniformity and sterility. Free (unentrapped) extract was separated by dialysis against 150-fold excess PBS over 24 hours using a dialysis membrane (MWCO 12,000 Da), with the dialysate replaced at 4-hour intervals (33, 34).

Determination of Maximum Absorption Wavelength and Standard Curves

The UV-Vis absorption spectrum of Ashwagandha extract was recorded from 200 to 800 nm in 10 nm increments using a UV-Vis spectrophotometer. A maximum absorption wavelength (λmax) of 240 nm was established. Calibration curves were constructed in two solvent systems: isopropanol (for quantification of encapsulated extract) and PBS pH 7.4 (for quantification of released extract). Serial dilutions of Ashwagandha extract were prepared and absorbance measured at 240 nm. All standard curves exhibited $R^2 \geq 0.98$, confirming linearity over the tested concentration range (35).

Encapsulation Efficiency

Encapsulation efficiency (EE%) was determined indirectly. After dialysis, niosomal suspension was disrupted with isopropanol (1:1 v/v) to release encapsulated extract. Absorbance was measured at 240 nm and the total encapsulated drug concentration was calculated from the isopropanol standard curve. EE% was calculated as: EE% = (Amount of

https://doi.org/10.22034/jrb.2026.07.V2I1A1

encapsulated extract / Total amount of extract added) × 100.

In Vitro Drug Release Studies

Drug release kinetics were studied under two simulated physiological conditions to reflect the normal tissue environment and the tumour microenvironment: (i) PBS pH 7.4 at 37°C (normophysiological conditions) and (ii) PBS pH 5.2 at 42°C (simulating the acidic, hyperthermic tumour milieu). Niosomal suspension was placed in a dialysis bag (MWCO 12,000 Da) and dialysed against 150 mL of the respective release medium under continuous stirring. At predetermined time intervals (1, 2, 4, 8, 16, 24, 48, and 72 hours), 3 mL aliquots were withdrawn and replaced with an equal volume of fresh medium. Absorbance was measured at 240 nm and cumulative release was calculated from the PBS standard curve. Statistical significance of differences in release profiles at 37°C and 42°C was assessed by one-way ANOVA (36).

Physicochemical Characterisation

The hydrodynamic diameter, polydispersity index (PDI), and zeta potential of niosome nanoparticles were measured by dynamic light scattering (DLS) and electrophoretic light scattering using a Brookhaven ZetaPlus analyser (Brookhaven Instruments Corporation, USA). All measurements were performed in triplicate at 25°C. Fourier-transform infrared (FTIR) spectroscopy was performed on lyophilised niosome samples (drug-free and drug-loaded) over the range 400–4000 cm^{-1} to assess potential drug–excipient interactions (37, 38).

Physical Stability Assessment

The physical stability of the optimised niosomal formulation was evaluated over 60 days at 4°C. Particle size, PDI, zeta potential, and encapsulation efficiency were measured at 0, 15, 30, and 60 days. Changes relative to the freshly prepared formulation were assessed by one-way ANOVA; $P > 0.05$ was considered indicative of no significant change.

Cell Culture

HeLa (human cervical carcinoma) and HFF (human skin fibroblast) cells were maintained in Dulbecco's Modified Eagle's Medium (DMEM) supplemented with 10% heat-inactivated FBS, 2 mM L-glutamine, 100 U/mL penicillin, and 100 µg/mL streptomycin, in a humidified incubator at 37°C with 5% CO_2. Cells were passaged at 70–80% confluence using 0.25% trypsin-EDTA (39, 40).

MTT Cytotoxicity Assay

Cytotoxicity was evaluated by the MTT (3-(4,5-dimethylthiazol-2-yl)-2,5 diphenyltetrazolium bromide) colorimetric assay. Cells were seeded in 96-well plates at a density of 10,000 cells/well and allowed to adhere for 24 hours. Cells were then treated with serial concentrations of free Ashwagandha extract, Ashwagandha-loaded niosomes, or empty niosomes (20, 40, 80, 160, and 320 µg/mL) for 48 hours. After incubation, medium was aspirated and 100 µL of MTT solution (0.5 mg/mL in PBS) was added per well. Following 3–4 hours of incubation at 37°C, the formazan crystals were solubilised in 100 µL DMSO, and absorbance was recorded at 570 nm using a Bio-Tek microplate spectrophotometer (USA). Cell viability (%) = (Absorbance of treated cells / Absorbance of control cells) × 100. The half-maximal inhibitory concentration (IC50) was derived from dose-

response curves using non-linear regression (41).

Real-Time PCR Gene Expression Analysis

HeLa cells were seeded in 6-well plates and treated with free extract, empty niosomes, or Ashwagandha-loaded niosomes at concentrations of 100, 250, and 500 µg/mL for 24 hours. Total RNA was isolated using the RNX-Plus reagent following the manufacturer's protocol. Complementary DNA (cDNA) was synthesised by reverse transcription. Real-Time PCR was performed over 35 cycles using EvaGreen-based chemistry with the following thermal cycling conditions: initial denaturation at 95°C for 5 minutes; followed by 35 cycles of denaturation at 95°C for 30 seconds, annealing at 80°C for 30 seconds, and extension at 72°C for 30 seconds; with a final extension at 72°C for 5 minutes. Relative gene expression was calculated using the $2^{-++}Ct$ method, with β-actin as the housekeeping reference gene. Primer sequences are listed in Table 1 (42).

Statistical Analysis

All experiments were performed in triplicate and results expressed as mean ± standard deviation (SD). Statistical analyses were performed using PRISM software. Group comparisons were made by one-way or two-way ANOVA followed by Tukey's post-hoc test. A P-value < 0.05 was considered statistically significant. Differences in gene expression were assessed relative to the untreated control group (43). Statistical significance indicators are defined as follows: *P < 0.05, **P < 0.01, ***P < 0.001; ns = not significant.

Results

Formulation Selection and Encapsulation Efficiency

The optimal niosomal formulation (F7) was selected based on the highest encapsulation efficiency (EE) and favourable physicochemical characteristics. As summarised in Table 2, the EE of the optimised niosomes was 69 ± 2.8%, with a mean particle diameter of 101.2 nm, a PDI of 0.429, a zeta potential of −24.1 mV, and a maximum cumulative release of 60.7% over 72 hours.

Standard Curves and Spectrophotometric Characterisation

Based on the direct relationship between concentration and absorbance according to the Beer-Lambert law, a calibration curve for the drug containing ginseng extract was prepared in isopropanol solution and phosphate-buffered saline. This curve was plotted using the standard series method at a peak wavelength of 240 nm (Fig. 1). Additionally, a linear equation was defined for the drug to be used in calculations related to extract loading and release. The mentioned curves had a coefficient of determination (R^2) above 0.98 (Fig. 2). Based on the standard curve, the drug loading amount in niosomal nanoparticles containing the extract was reported as 69%.

In Vitro Drug Release Kinetics

The cumulative release profiles of Ashwagandha extract from niosomal formulations at two pH and temperature combinations are illustrated in Fig. 3 and 4. At pH 7.4 and 37°C (simulating normal physiological tissue), release followed a

https://doi.org/10.22034/jrb.2026.07.V2I1A1

Table 1. Primers sequences used for Real time PCR

Gene	Forward Primer (5′→3′)	Reverse Primer (5′→3′)
BCL2	ATCGCCCTGTGGATGACTGAGT	GCCAGGAGAAATCAAACAGAGGC
TP53	CCTCAGCATCTTATCCGAGTGG	TGGATGGTGGTACAGTCAGAGC
ACTB	AGACGCAGGATGGCATGG	GAGACCTTTCAACACCCCAGCC

Table 2. Physicochemical characterisation parameters of the optimised Ashwagandha-loaded niosomal formulation (F7).

Size (nm)	PDI	Zeta (mV)	EE% (Mean±SD)	Release (72h, %)
101.2	0.429	−24.1	69 ± 2.8	60.7

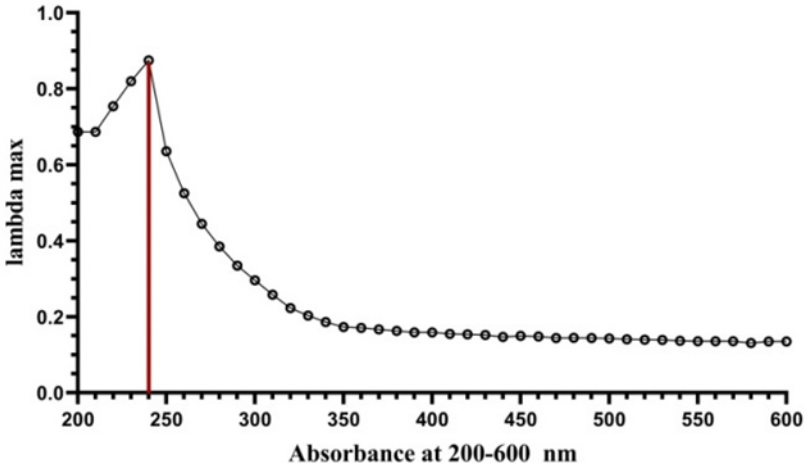

Figure 1. Investigation of lambda max of Ashwagandha (Ginseng) extract using spectrophotometry.

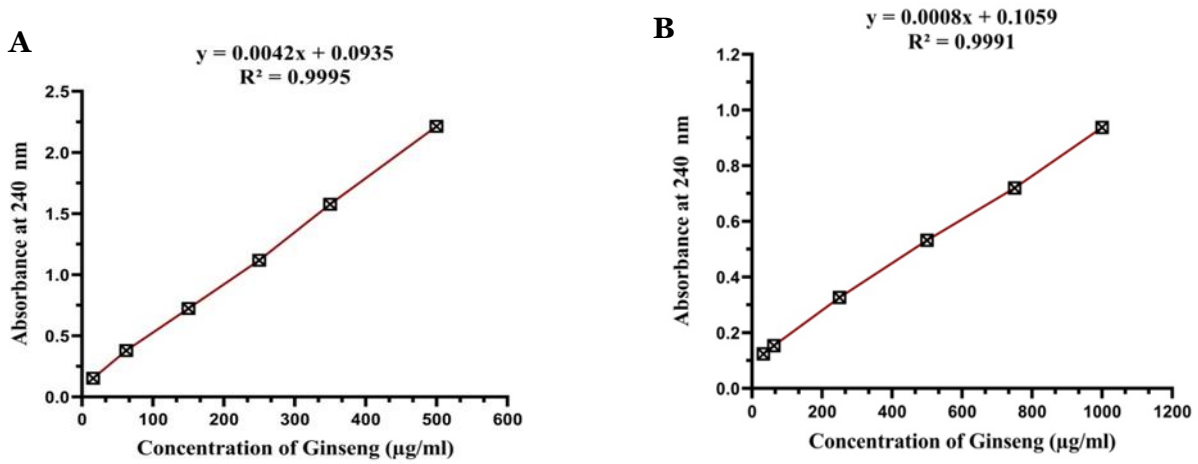

Figure 2. Standard calibration curves of Ashwagandha extract absorbance versus concentration at λmax = 240 nm: (A) in isopropanol for encapsulation efficiency determination; (B) in PBS pH 7.4 for in vitro drug release quantification. Both curves exhibit $R^2 \geq 0.98$.

biphasic pattern: a rapid initial burst phase during the first 8 hours (~35% release), succeeded by a sustained, near-linear phase over the subsequent 64 hours, reaching 60.7% at 72 hours. At pH 5.2 and 42°C (simulating tumour microenvironment conditions), release was significantly accelerated throughout: burst release reached approximately 42% at 8 hours, with cumulative release at 72 hours reaching ~75%. This pH- and temperature-responsive release behaviour is consistent with the known susceptibility of niosomal bilayers to acid-induced swelling and hydrolytic disruption of non-ionic surfactant ester bonds. The sustained-release profile, with preferential acceleration under tumour-mimicking conditions, provides a mechanistic rationale for the selective anti-tumour activity of this nanoformulation.

Hydrodynamic Diameter, Zeta Potential, and Polydispersity Index

DLS analysis of the optimised formulation (F7) yielded a mean hydrodynamic diameter of 101.2 nm and a zeta potential of −24.1 mV, with a PDI of 0.429. A particle size below 200 nm is widely regarded as optimal for passive tumour targeting via the EPR effect, enabling preferential accumulation in tumour vasculature while limiting uptake by the mononuclear phagocyte system. The negative zeta potential of −24.1 mV indicates adequate electrostatic repulsion between nanoparticles, conferring colloidal stability and minimising aggregation in aqueous suspension.

FTIR Spectroscopic Analysis

FTIR spectra of drug-free and Ashwagandha-loaded niosomes are presented in Fig. 5. The drug-free niosomal formulation displayed characteristic absorption peaks at 3326 cm^{-1} (O–H stretching), 2126 cm^{-1} (C=C aromatic stretching), 1636 cm^{-1} (C=O carbonyl stretching), and 620 cm^{-1} (C–O stretching). The loaded niosomes exhibited corresponding peaks at 3337, 2125, 1635, and 618 cm^{-1}. The marginal shifts in peak positions (< 10 cm^{-1}) and the absence of new absorption bands in the drug-loaded formulation indicate that the Ashwagandha extract was physically incorporated into the niosomal bilayer without chemical interaction or covalent modification of either the extract components or the niosomal matrix**.**

Colloidal Stability Over 60 Days

Physical stability of the niosomal formulation was monitored over 60 days at 4°C. As shown in Fig. 6, no statistically significant changes in particle size, PDI, or zeta potential were observed at 15, 30, or 60 days compared to freshly prepared niosomes ($P > 0.05$ for all parameters). These results indicate excellent long-term colloidal stability of the Ashwagandha-loaded niosomal system. A modest, statistically significant reduction in drug loading was noted at 60 days ($P < 0.05$), attributed to slow passive leakage of extract through the niosomal bilayer during prolonged storage, a phenomenon commonly reported for plant extract-loaded vesicular systems.

Cytotoxicity Evaluation by MTT Assay

The cytotoxic effects of free Ashwagandha extract, Ashwagandha-loaded niosomes, and empty niosomes on HeLa cervical cancer cells and normal HFF fibroblasts were evaluated after 48 hours of treatment. Both free and niosomal Ashwagandha significantly inhibited HeLa cell proliferation in a concentration-dependent manner (Fig. 7).

https://doi.org/10.22034/jrb.2026.07.V2I1A1

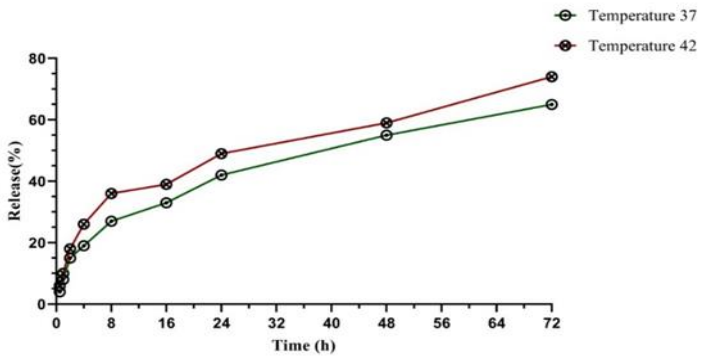

Figure 3. In vitro cumulative release profiles of *Ashwagandha* extract from niosomal nanoparticles over 72 hours at two simulated microenvironments: pH 7.4 / 37°C (normal physiological conditions) and pH 5.2 / 42°C (tumour microenvironment conditions). Data represent mean ± SD (n = 3). The niosomal system demonstrates pH- and temperature-responsive drug release.

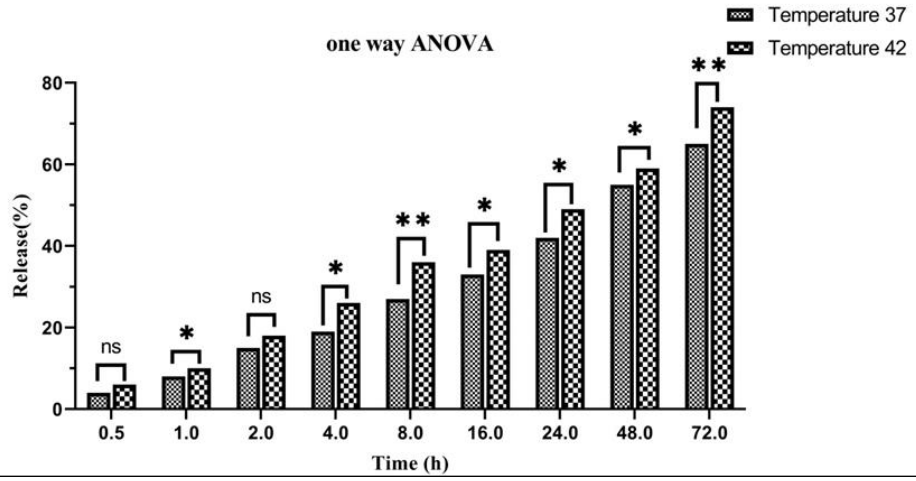

Figure 4. Comparison of *Ashwagandha* extract release from niosomal nanoparticles at 37°C versus 42°C at various time points. Data represent mean ± SD (n = 3). (*P < 0.05; ns = not significant). Release at 42°C was significantly greater than at 37°C at 24, 48, and 72 hours.

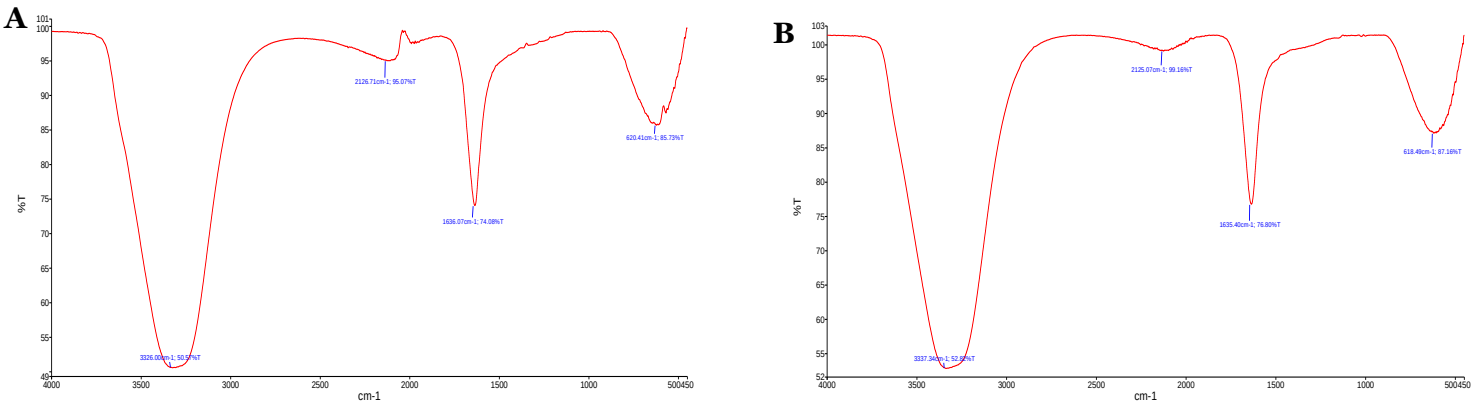

Figure 5. FTIR spectra of (A) drug-free and (B) *Ashwagandha*-loaded niosomal nanoparticles. Characteristic peaks at 3326 cm^{-1} (O–H stretch), 2126 cm^{-1} (C=C aromatic), 1636 cm^{-1} (C=O carbonyl), and 620 cm^{-1} (C–O stretch) confirm the niosomal bilayer composition. Peak positions are minimally shifted in drug-loaded niosomes (< 10 cm^{-1}), confirming physical encapsulation without chemical interaction between the extract and the niosomal excipients.

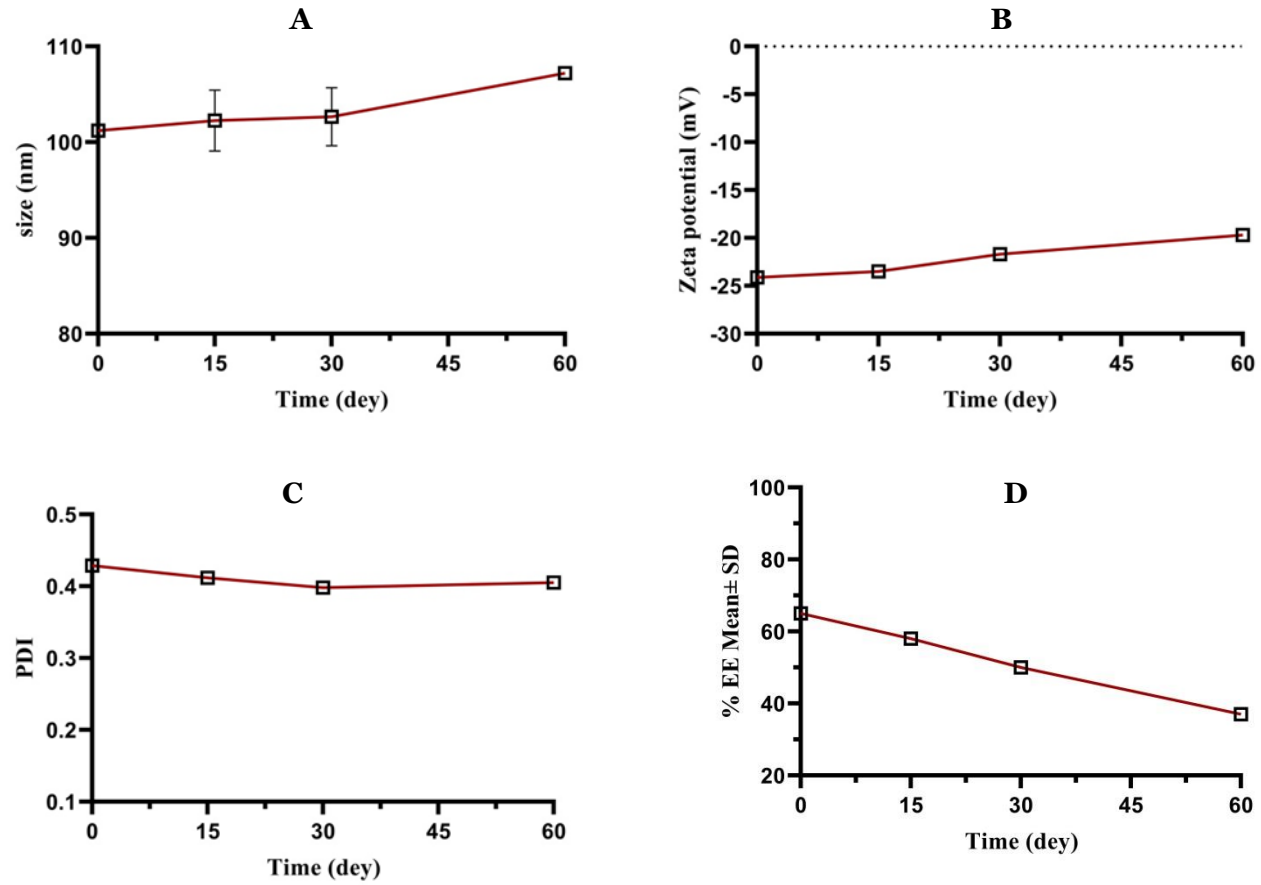

Figure 6. Stability profiles of *Ashwagandha* extract-loaded niosomal nanoparticles stored at 4°C over 60 days: (A) particle size (nm); (B) zeta potential (mV); (C) polydispersity index (PDI); (D) encapsulation efficiency (%). Data represent mean ± SD (n = 3). No significant changes in size, zeta potential, or PDI were observed over the study period ($P > 0.05$); drug loading showed a modest but statistically significant decrease at 60 days ($P < 0.05$).

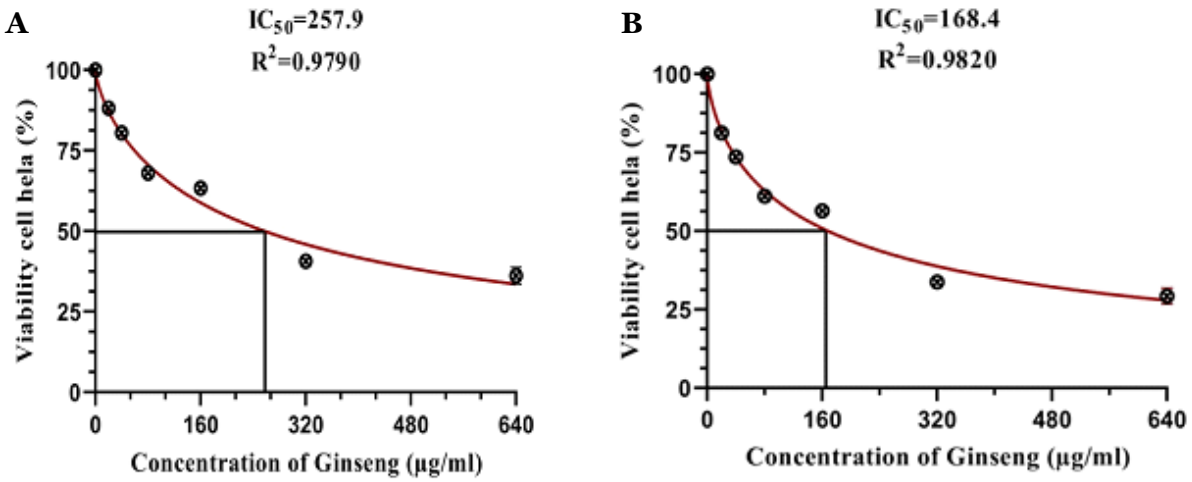

Figure 7. Dose-response curves and IC50 determination for (A) free *Ashwagandha* extract and (B) *Ashwagandha*-loaded niosomal nanoparticles against HeLa cervical cancer cells after 48 hours. The niosomal formulation demonstrates a markedly lower IC50 (168 µg/mL) compared to the free extract (257.9 µg/mL).

https://doi.org/10.22034/jrb.2026.07.V2I1A1

and 8). The IC50 of the niosomal formulation against HeLa cells (168 µg/mL) was substantially lower than that of the free extract (257.9 µg/mL), representing a 1.5-fold and 8). The IC50 of the niosomal formulation against HeLa cells (168 µg/mL) was substantially lower than that of the free extract (257.9 µg/mL), representing a 1.5-fold improvement in anti-cancer potency attributable to enhanced cellular uptake and retention facilitated by the nanocarrier. Empty niosomes at equivalent concentrations (20–320 µg/mL) had no significant effect on HeLa cell viability (Figure 9A; $P > 0.05$ vs. untreated control), confirming that the cytotoxic activity was attributable exclusively to the encapsulated *Ashwagandha* extract and not to the niosomal vehicle itself. In normal HFF fibroblasts, both free and niosomal Ashwagandha extract showed substantially reduced cytotoxicity compared to HeLa cells at equivalent concentrations (Fig. 9B; $P < 0.05$), demonstrating a favourable therapeutic index and selective anti-cancer activity, consistent with the concept of EPR effect-mediated tumour selectivity.

Real-Time PCR Gene Expression Analysis

Expression of BCL2 and TP53 genes in HeLa cells was quantified by Real-Time PCR following 24-hour treatment with free extract, empty niosomes, and *Ashwagandha*-loaded niosomes at 100, 250, and 500 µg/mL. The melting curve of the GAPDH reference gene (Fig. 10) confirmed the specificity of PCR amplification. Both free and niosomal Ashwagandha extract produced concentration-dependent upregulation of TP53 and downregulation of BCL2 expression relative to the untreated control group (Fig. 11 and 12). Crucially, the magnitude of these gene expression changes was significantly greater for the niosomal formulation compared to the free extract at all concentrations tested ($P < 0.05$). At 500 µg/mL, niosomal *Ashwagandha* induced TP53 expression to approximately 3.2-fold above control levels, compared to 1.8-fold for the free extract. Correspondingly, BCL2 expression was suppressed to approximately 30% of control levels by niosomal *Ashwagandha*, compared to 55% by the free extract. Empty niosomes produced no significant changes in BCL2 or TP53 expression. These results are mechanistically consistent with the MTT cytotoxicity data and support the conclusion that the niosomal formulation enhances intracellular delivery of bioactive *Ashwagandha* compounds, amplifying their pro-apoptotic effects.

Discussion

The present study successfully developed and characterized niosomal nanoparticles loaded with *Withania somnifera* extract for potential application in cervical cancer therapy. The results demonstrate that the niosomal formulation exhibits favorable physicochemical properties, controlled drug release behavior, selective cytotoxicity against HeLa cervical cancer cells, and modulation of key apoptotic regulatory genes, including BCL2 and TP53. The choice of non-ionic surfactant and cholesterol ratio is critical for the formation of stable niosomes with optimal drug encapsulation and release properties (44). In this study, Span-60 (sorbitan monostearate) was selected as the non-ionic surfactant due to its biocompatibility, biodegradability, and ability to form stable vesicular structures.

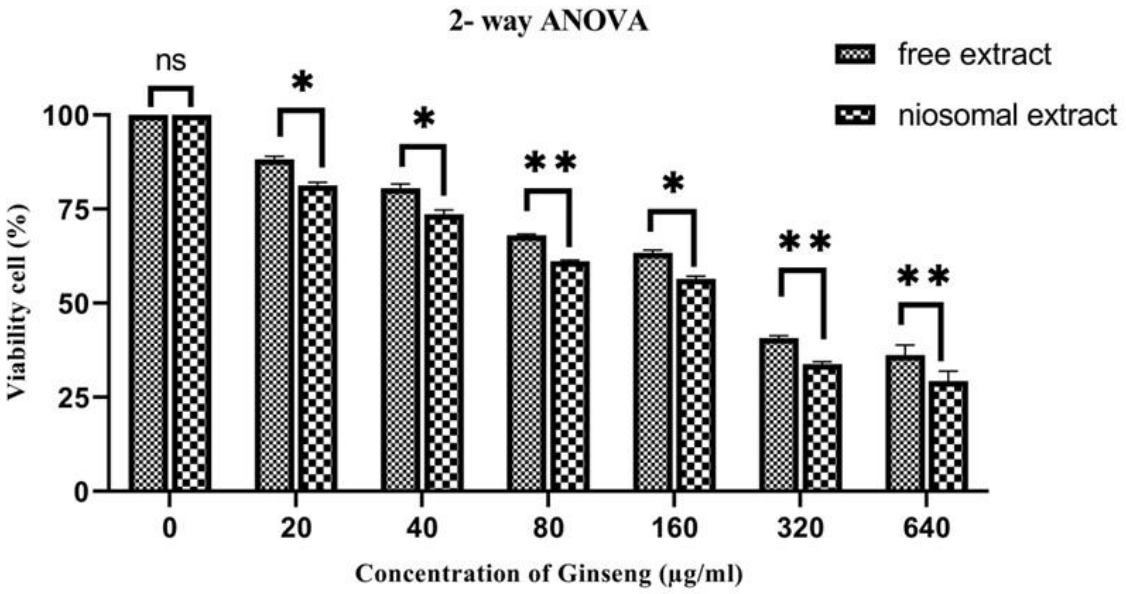

Figure 8. Comparative cell viability (%) of HeLa cells after 48-hour exposure to free *Ashwagandha* extract and *Ashwagandha*-loaded niosomes at concentrations of 20–320 µg/mL. (*P < 0.05; ns = not significant). Niosomal extract demonstrated significantly greater cytotoxicity than the free extract at concentrations ≥ 80 µg/mL.

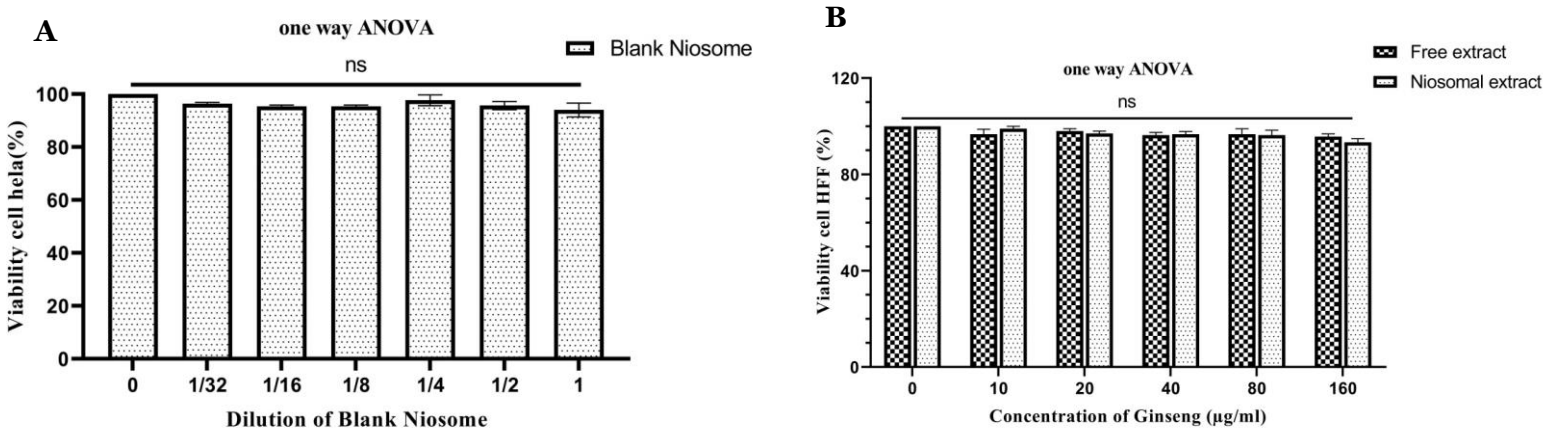

Figure 9. (A) Cell viability (%) of HeLa cells after 48-hour treatment with empty (drug-free) niosomal nanoparticles at concentrations of 20–320 µg/mL. Empty niosomes exhibited no significant cytotoxicity compared to untreated controls at all concentrations tested (P > 0.05; ns = not significant), confirming biocompatibility of the niosomal carrier. (B) Cell viability (%) of normal human skin fibroblast (HFF) cells following 48-hour treatment with free and niosomal *Ashwagandha* extract. Both formulations demonstrated significantly reduced toxicity toward normal cells compared to HeLa cancer cells (*P < 0.05), indicating selective anti-tumour activity and a favourable therapeutic index.

https://doi.org/10.22034/jrb.2026.07.V2I1A1

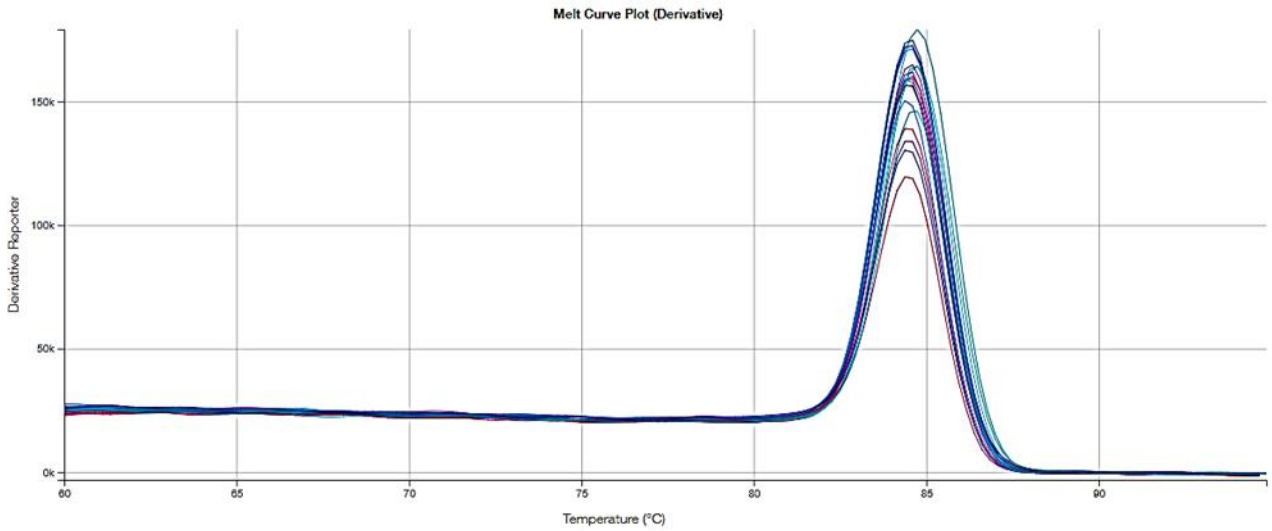

Figure 10. Melting curve analysis for GAPDH (housekeeping reference gene) used in Real-Time PCR experiments. A single sharp peak confirms amplification specificity and absence of non-specific products or primer-dimers.

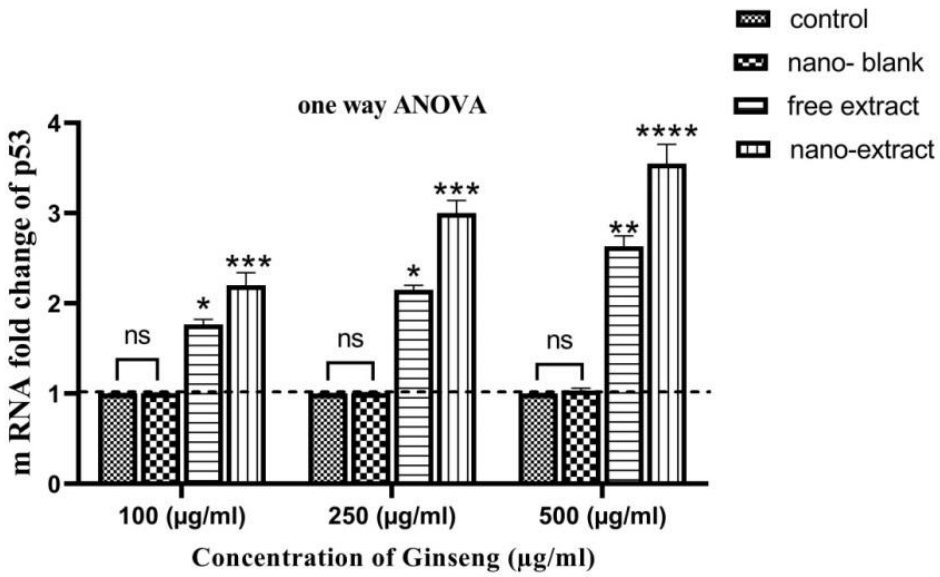

Figure 11. Relative expression of TP53 gene in HeLa cells following 24-hour treatment with free Ashwagandha extract, empty niosomes, and *Ashwagandha*-loaded niosomes at 100, 250, and 500 µg/mL, determined by Real-Time PCR (2^{-++}Ct method; β-actin reference). Niosomal *Ashwagandha* significantly upregulated TP53 expression compared to free extract (*P < 0.05; ns = not significant).

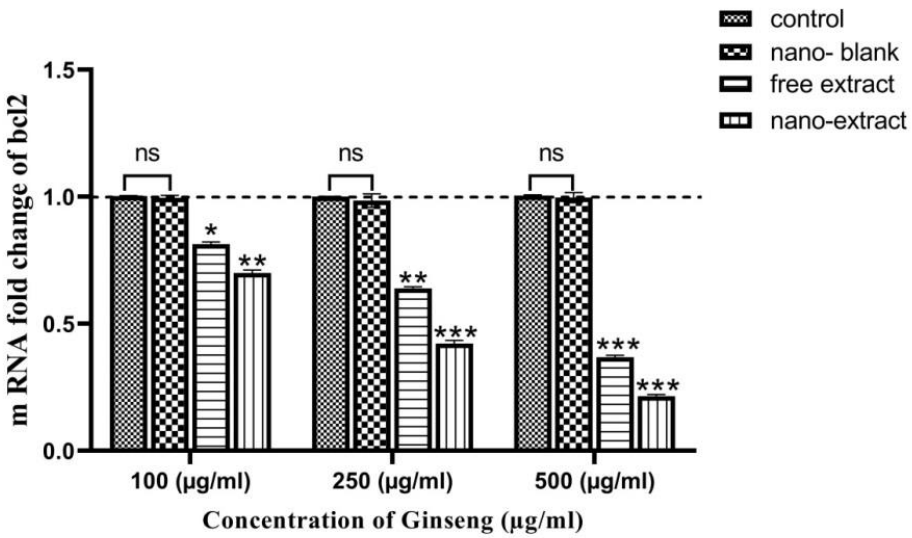

Figure 12. Relative expression of BCL2 gene in HeLa cells following 24-hour treatment with free *Ashwagandha* extract, empty niosomes, and Ashwagandha-loaded niosomes at 100, 250, and 500 µg/mL, determined by Real-Time PCR (2^{-++}Ct method; β-actin reference). Niosomal *Ashwagandha* significantly downregulated BCL2 expression compared to free extract (*P < 0.05; ns = not significant).

Cholesterol was incorporated into the niosomal formulation to enhance membrane rigidity, reduce drug leakage, and improve the stability of the vesicles (45, 46). The optimization studies revealed that the formulation with a Span-60:cholesterol ratio of 70:30 exhibited the most favorable properties in terms of particle size, polydispersity index (PDI), zeta potential, and encapsulation efficiency. This ratio provided an optimal balance between membrane fluidity and rigidity, allowing for efficient encapsulation of the *Withania somnifera* extract while maintaining vesicle stability. The particle size of nanocarriers is a crucial parameter that influences their biodistribution, cellular uptake, and tumor penetration (47). The optimized niosomal formulation exhibited a mean particle size of approximately 101 nm with a narrow size distribution, indicating good homogeneity.

Nanoparticles in the size range of 100-200 nm are considered optimal for cancer therapy due to their ability to exploit the enhanced permeability and retention (EPR) effect, which allows for preferential accumulation in tumor tissues through leaky tumor vasculature (48). The zeta potential of the niosomal formulation was measured to be approximately -25 mV, indicating good colloidal stability. A zeta potential with an absolute value greater than 20 mV is generally considered sufficient to prevent particle aggregation through electrostatic repulsion (49). The in vitro drug release profile of the niosomal formulation was evaluated under different pH conditions to simulate the physiological pH of blood (pH 7.4) and the acidic tumor microenvironment (pH 5.2). The results demonstrated a pH-dependent release pattern, with significantly higher drug release at acidic pH compared to

https://doi.org/10.22034/jrb.2026.07.V2I1A1

physiological pH. This pH-sensitive release behavior is highly desirable for cancer therapy, as it allows for preferential drug release in the acidic tumor microenvironment while minimizing premature drug release in the bloodstream and normal tissues (29, 30). The drug release kinetics were analyzed using various mathematical models, including zero-order, first-order, Higuchi, and Korsmeyer-Peppas models. The release data best fitted the Korsmeyer-Peppas model, suggesting that the drug release mechanism involves a combination of diffusion and erosion processes. The cytotoxic effects of free *Withania somnifera* extract and niosomal formulation were evaluated against HeLa cervical cancer cells and normal fibroblast cells using the MTT assay. The results demonstrated that both free extract and niosomal formulation exhibited dose-dependent cytotoxicity against HeLa cells. However, the niosomal formulation showed significantly higher cytotoxic activity compared to the free extract, with a lower IC50 value. The enhanced cytotoxicity of the niosomal formulation can be attributed to several factors: (1) improved cellular uptake of the nanoparticles through endocytosis mechanisms; (2) protection of the bioactive compounds from degradation in the extracellular environment; (3) sustained and controlled release of the extract within the cells; and (4) enhanced accumulation of the drug in cancer cells due to the EPR effect (50). Importantly, the niosomal formulation exhibited selective cytotoxicity toward cancer cells, with significantly lower toxicity against normal fibroblast cells. This selective cytotoxicity is a crucial advantage over conventional chemotherapeutic agents, which often cause severe side effects due to non-specific toxicity to normal cells. The selective toxicity of the niosomal formulation may be attributed to the preferential uptake of nanoparticles by cancer cells due to their higher metabolic activity and the EPR effect, as well as the inherent selectivity of withanolides toward cancer cells (51). To elucidate the molecular mechanisms underlying the anticancer effects of the niosomal formulation, the expression levels of BCL2 and TP53 genes were analyzed using quantitative real-time PCR (qRT-PCR). BCL-2 is an anti-apoptotic protein that plays a critical role in preventing apoptosis by inhibiting mitochondrial outer membrane permeabilization and the release of cytochrome c (9). Overexpression of BCL-2 is commonly observed in various cancers, including cervical cancer, and is associated with resistance to chemotherapy and poor prognosis (10). The results demonstrated that treatment with the niosomal formulation significantly downregulated BCL2 gene expression in HeLa cells in a dose-dependent manner. This downregulation of BCL-2 suggests that the niosomal formulation promotes apoptosis by reducing the expression of anti-apoptotic proteins, thereby shifting the balance toward pro-apoptotic signals and facilitating mitochondrial-mediated apoptosis. In contrast, the expression of p53, a tumor suppressor protein that plays a central role in regulating cell cycle arrest, DNA repair, and apoptosis, was significantly upregulated following treatment with the niosomal formulation (11). This upregulation of p53 is particularly significant in the context of cervical cancer, where HPV E6 oncoprotein promotes the degradation of p53, leading to loss of its tumor suppressor functions (5). The ability of

the niosomal formulation to restore p53 expression suggests that *Withania somnifera* extract may interfere with the HPV E6-mediated degradation of p53 or enhance p53 transcription and translation. The simultaneous downregulation of BCL-2 and upregulation of p53 creates a synergistic pro-apoptotic environment that enhances the sensitivity of cancer cells to apoptotic stimuli.

The stability of the niosomal formulation was evaluated under different storage conditions over a period of 60 days. The results showed that the niosomes maintained their physicochemical properties, including particle size, PDI, zeta potential, and encapsulation efficiency, with minimal changes during storage at 4°C. The good stability of the niosomal formulation can be attributed to the presence of cholesterol, which enhances membrane rigidity and reduces drug leakage, as well as the non-ionic nature of the surfactant, which makes the vesicles less susceptible to hydrolysis and oxidation compared to phospholipid-based liposomes (44). The findings of this study are consistent with previous reports on the anticancer effects of *Withania somnifera* extracts and the advantages of nanoparticle-based delivery systems. The use of niosomal nanoparticles for the delivery of herbal extracts has been explored in several recent studies. For example, Hesampour et al. (2022) developed niosomal formulations of Artemisia turcomanic extract and demonstrated enhanced anticancer activity against HeLa cells (52). Similarly, Sahrayi et al. (2021) reported the successful co-delivery of letrozole and cyclophosphamide using folic acid-decorated niosomes for breast cancer therapy (53). These studies support the potential of niosomal systems for improving the therapeutic efficacy of natural products and chemotherapeutic agents. The present study extends these findings by demonstrating the specific molecular mechanisms through which niosomal *Withania somnifera* extract exerts its anticancer effects, particularly through modulation of BCL2 and TP53 expression. The downregulation of BCL-2 and upregulation of p53 represent key molecular events that contribute to the restoration of apoptotic sensitivity in cancer cells. These findings are particularly relevant for cervical cancer, where HPV-mediated inactivation of p53 is a major driver of carcinogenesis (54). However, several challenges and limitations need to be addressed before clinical translation. The present study was conducted using in vitro cell culture models, which do not fully recapitulate the complexity of the tumor microenvironment. Therefore, further studies using in vivo animal models are necessary to evaluate the pharmacokinetics, biodistribution, tumor accumulation, therapeutic efficacy, and safety profile of the niosomal formulation. Additionally, the standardization and quality control of herbal extracts remain a challenge due to the variability in the content of bioactive compounds depending on factors such as plant source, geographical location, harvesting time, and extraction methods (17). To ensure reproducibility and consistency of the therapeutic effects, it is essential to develop standardized extraction protocols and analytical methods for the quantification of key bioactive compounds, particularly withanolides.

Conclusion

This study demonstrates that niosomal encapsulation of Withania somnifera

https://doi.org/10.22034/jrb.2026.07.V2I1A1

(Ashwagandha) extract using Span-60 and cholesterol at a 70:30 molar ratio via the thin-film hydration method yields nanoparticles with favourable physicochemical properties (size ~101 nm, zeta potential −24 mV, EE 69%), sustained and pH/temperature-responsive drug release, and excellent colloidal stability over 60 days. The niosomal formulation exhibited markedly enhanced anti-tumour potency against HeLa cervical cancer cells (IC50 168 µg/mL vs. 257.9 µg/mL for free extract) with selective cytotoxicity toward cancer cells and negligible toxicity to normal fibroblasts. Mechanistically, the formulation significantly upregulated p53 and downregulated BCL-2 expression in HeLa cells, confirming induction of the intrinsic apoptotic pathway. These findings establish Ashwagandha-loaded niosomes as a biocompatible, efficacious, and mechanistically rational nanoplatform for cervical cancer therapy, warranting further evaluation in vivo and progression toward clinical development.

Conflict of Interest

The authors declare no conflict of interest.

Acknowledgements

The authors express their gratitude to the University of Science and Art (Iran) for institutional support, and to the Yazd Infertility Center for providing HFF cell lines.

References

1. Siegel RL, Miller KD, Jemal A. Cancer statistics, 2018. CA Cancer J Clin. 2018;68(1):7-30.

2. Cohen PA, Jhingran A, Oaknin A, Denny L. Cervical cancer. Lancet. 2019;393(10167):169-82.

3. Dunne EF, Park IU. HPV and HPV-associated diseases. Infect Dis Clin North Am. 2013;27(4):765-78.

4. Ghittoni R, Accardi R, Hasan U, Gheit T, Sylla B, Tommasino M. The biological properties of E6 and E7 oncoproteins from human papillomaviruses. Virus Genes. 2010;40:1-13.

5. Martinez-Zapien D, Ruiz FX, Poirson J, Mitschler A, Ramirez J, Forster A, et al. Structure of the E6/E6AP/p53 complex required for HPV-mediated degradation of p53. Nature. 2016;529(7587):541-5.

6. Ahlberg K, Ekman T, Gaston-Johansson F. The experience of fatigue, other symptoms and global quality of life during radiotherapy for uterine cancer. Int J Nurs Stud. 2005;42(4):377-86.

7. Syeda S, Chen L, Hou JY, Tergas AI, Khoury-Collado F, Melamed A, et al. Chemotherapy, radiation, or combination therapy for stage III uterine cancer. Obstet Gynecol. 2019;134(1):17.

8. Chen Z, Ling K, Zhu Y, Deng L, Li Y, Liang Z. Rucaparib antagonizes multidrug resistance in cervical cancer cells through blocking the function of ABC transporters. Gene. 2020;759:145000.

9. Hardwick JM, Youle RJ. SnapShot: BCL-2 proteins. Cell. 2009;138(2):404.

10. Placzek W, Wei J, Kitada S, Zhai D, Reed J, Pellecchia M. A survey of the anti-apoptotic Bcl-2 subfamily expression in cancer types provides a platform to predict the efficacy of Bcl-2 antagonists in cancer therapy. Cell Death Dis. 2010;1(5):e40.

11. Kruse JP, Gu W. Modes of p53 regulation. Cell. 2009;137(4):609-22.

12. Olaku O, White JD. Herbal therapy use by cancer patients: a literature review on case reports. Eur J Cancer. 2011;47(4):508-14.

13. Potenza MA, Montagnani M, Santacroce L, Charitos IA, Bottalico L. Ancient herbal therapy: a brief history of Panax ginseng. J Ginseng Res. 2023;47(3):359-65.

14. Kulkarni S, Dhir A. Withania somnifera: an Indian ginseng. Prog Neuropsychopharmacol Biol Psychiatry. 2008;32(5):1093-105.

15. Mishra LC, Singh BB, Dagenais S. Scientific basis for the therapeutic use of Withania somnifera

(ashwagandha): a review. Altern Med Rev. 2000;5(4):334-46.

16. Sharifi-Rad J, Quispe C, Ayatollahi SA, Kobarfard F, Staniak M, Stępień A, et al. Chemical composition, biological activity, and health-promoting effects of Withania somnifera for pharma-food industry applications. J Food Qual. 2021;2021:1-14.

17. Ahmad M, Dar NJ. Withania somnifera: ethnobotany, pharmacology, and therapeutic functions. In: Sustained energy for enhanced human functions and activity. Elsevier; 2017. p. 137-54.

18. Dar NJ, Hamid A, Ahmad M. Pharmacologic overview of Withania somnifera, the Indian ginseng. Cell Mol Life Sci. 2015;72:4445-60.

19. Farokhzad OC, Langer R. Impact of nanotechnology on drug delivery. ACS Nano. 2009;3(1):16-20.

20. Saeedi M, Eslamifar M, Khezri K, Dizaj SM. Applications of nanotechnology in drug delivery to the central nervous system. Biomed Pharmacother. 2019;111:666-75.

21. Demetzos C. Application of nanotechnology in drug delivery and targeting. In: Pharmaceutical Nanotechnology: Fundamentals and Practical Applications. 2016:77-145.

22. Ag Seleci D, Seleci M, Walter JG, Stahl F, Scheper T. Niosomes as nanoparticular drug carriers: fundamentals and recent applications. J Nanomater. 2016;2016.

23. Bartelds R, Nematollahi MH, Pols T, Stuart MC, Pardakhty A, Asadikaram G, et al. Niosomes, an alternative for liposomal delivery. PLoS One. 2018;13(4):e0194179.

24. Hemati H, Haghiralsadat F, Hemati M, Sargazi G, Razi N. Design and evaluation of liposomal sulforaphane loaded polyvinyl alcohol/polyethylene glycol (PVA/PEG) hydrogels as a novel drug delivery system for wound healing. Gels. 2023;9:748. doi:10.3390/gels9090748.

25. Gharbavi M, Johari B, Mousazadeh N, Rahimi B, Leilan MP, Eslami SS, et al. Hybrid of niosomes and bio-synthesized selenium nanoparticles as a novel approach in drug delivery for cancer treatment. Mol Biol Rep. 2020;47:6517-29.

26. Mehrarya M, Gharehchelou B, Haghighi Poodeh S, Jamshidifar E, Karimifard S, Farasati Far B, et al. Niosomal formulation for antibacterial applications. J Drug Target. 2022;30(5):476-93.

27. Akbarzadeh I, Farid M, Javidfar M, Zabet N, Shokoohian B, Arki MK, et al. The optimized formulation of tamoxifen-loaded niosomes efficiently induced apoptosis and cell cycle arrest in breast cancer cells. AAPS PharmSciTech. 2022;23(1):1-13.

28. Xu YQ, Chen WR, Tsosie JK, Xie X, Li P, Wan JB, et al. Niosome encapsulation of curcumin: characterization and cytotoxic effect on ovarian cancer cells. J Nanomater. 2016;2016.

29. Tila D, Yazdani-Arazi SN, Ghanbarzadeh S, Arami S, Pourmoazzen Z. pH-sensitive, polymer modified, plasma stable niosomes: promising carriers for anti-cancer drugs. EXCLI J. 2015;14:21.

30. Rinaldi F, Del Favero E, Rondelli V, Pieretti S, Bogni A, Ponti J, et al. pH-sensitive niosomes: effects on cytotoxicity and on inflammation and pain in murine models. J Enzyme Inhib Med Chem. 2017;32(1):538-46.

31. Akbarzadeh I, Saremi Poor A, Yaghmaei S, Norouzian D, Noorbazargan H, Saffar S, et al. Niosomal delivery of simvastatin to MDA-MB-231 cancer cells. Drug Dev Ind Pharm. 2020;46(9):1535-49.

32. Akbarzadeh I, Yaraki MT, Ahmadi S, Chiani M, Nourouzian D. Folic acid-functionalized niosomal nanoparticles for selective dual-drug delivery into breast cancer cells: an in-vitro investigation. Adv Powder Technol. 2020;31(9):4064-71.

33. Momo F, Fabris S, Stevanato R. Interaction of fluoxetine with phosphatidylcholine liposomes. Biophys Chem. 2005;118(1):15-21.

34. Katragadda A, Bridgman R, Betageri G. Effect of liposome composition and cholesterol on the cellular uptake of stavudine by human monocyte/macrophages. Cell Mol Biol Lett. 2000;5(4):483-94.

35. Akhlaghi M, Taebpour M, Lotfabadi NN, Naghib SM, Jalili N, Farahmand L, et al. Synthesis and characterization of smart stimuli-responsive herbal drug-encapsulated nanoniosome particles for efficient

https://doi.org/10.22034/jrb.2026.07.V2I1A1

treatment of breast cancer. Nanotechnol Rev. 2022;11(1):1364-85.

36. Siyadatpanah A, Norouzi R, Mirzaei F, et al. Green synthesis of nano liposomes containing Bunium persicum and Trachyspermum ammi essential oils against Trichomonas vaginalis. J Microbiol Immunol Infect. 2022. doi:10.1016/j.jmii.2022.06.006.

37. Kuhn MA, Winston D. Herbal therapy and supplements: a scientific and traditional approach. Philadelphia: Lippincott Williams & Wilkins; 2000.

38. Ghim SJ, Basu PS, Jenson AB. Cervical cancer: etiology, pathogenesis, treatment, and future vaccines. Asian Pac J Cancer Prev. 2002;3(3):207-14.

39. Fonseca-Moutinho JA. Smoking and cervical cancer. ISRN Obstet Gynecol. 2011;2011:847684.

40. Messiou C, Morgan VA, De Silva SS, Ind TE, deSouza NM. Diffusion weighted imaging of the uterus: regional ADC variation with oral contraceptive usage and comparison with cervical cancer. Acta Radiol. 2009;50(6):696-701.

41. Kashyap N, Krishnan N, Kaur S, Ghai S. Risk factors of cervical cancer: a case-control study. Asia Pac J Oncol Nurs. 2019;6(3):308-14.

42. Mishra GA, Pimple SA, Shastri SS. An overview of prevention and early detection of cervical cancers. Indian J Med Paediatr Oncol. 2011;32(03):125-32.

43. Kasi D, HC H, RP P, Sayeeda D. Cervical cancer: an overview. IOSR J Dent Med Sci. 2021;20(5).

44. Esmaeilzadeh AA, Nasirzadeh F. Uterus cancer. Eurasian J Chem Med Petrol Res. 2023;2(5):63-83.

45. Arbyn M, Weiderpass E, Bruni L, de Sanjosé S, Saraiya M, Ferlay J, et al. Estimates of incidence and mortality of cervical cancer in 2018: a worldwide analysis. Lancet Glob Health. 2020;8(2):e191-203.

46. Condrat CE, Filip L, Gherghe M, Cretoiu D, Suciu N. Maternal HPV infection: Effects on pregnancy outcome. Viruses. 2021;13(12):2455.

47. De Luca P, Moiola CP, Zalazar F, Gardner K, Vazquez ES, De Siervi A. BRCA1 and p53 regulate critical prostate cancer pathways. Prostate Cancer Prostatic Dis. 2013;16(3):233-8.

48. Amoabediny G, Haghiralsadat F, Naderinezhad S, Helder MN, Akhoundi Kharanaghi E, Mohammadnejad Arough J, ZandiehDoulabi B. Overview of preparation methods of polymeric and lipid based (niosomal, solid lipid, liposomal) nanoparticles: a comprehensive review. Int J Polym Mater Polym Biomater. 2017. doi:10.1080/00914037.2017.1332623.

49. Hesampour A. Preparation of Artemisia turcomanic encapsulated niosomal nanocarrier and evaluation of anti-cancer activities and apoptosis gene expression analysis in uterine cancer cell lines (Hela). [Thesis]. 2022.

50. Sahrayi H, Hosseini E, Karimifard S, Khayam N, Meybodi SM, Amiri S, et al. Co-delivery of letrozole and cyclophosphamide via folic acid-decorated nanoniosomes for breast cancer therapy. Pharmaceuticals. 2021;15(1):6.

51. Siegel RL, Miller KD, Jemal A. Cancer statistics, 2019. CA Cancer J Clin. 2019;69(1):7-34.

52. Hesampour A. Preparation of Artemisia turcomanic encapsulated niosomal nanocarrier and evaluation of anti-cancer activities and apoptosis gene expression analysis in uterine cancer cell lines (Hela). [Thesis]. 2022.

53. Sahrayi H, Hosseini E, Karimifard S, Khayam N, Meybodi SM, Amiri S, et al. Co-delivery of letrozole and cyclophosphamide via folic acid-decorated nanoniosomes for breast cancer therapy. Pharmaceuticals. 2021;15(1):6.

54. De Luca P, Moiola CP, Zalazar F, Gardner K, Vazquez ES, De Siervi A. BRCA1 and p53 regulate critical prostate cancer pathways. Prostate Cancer Prostatic Dis. 2013;16(3):233-8.